A C T A U N I V E R S I T A T I S L O D Z I E N S I S
FOLIA BIOCHIMICA ET BIOPHYSICA 5, 1986

G. Buso, P. Colautti, G. Moschini, B. M. Stievano

A NUCLEAR TECHNIQUE FOR THE ELEMENTAL QUANTITATIVE ANALYSIS: THE PROTON-INDUCED X-RAY EMISSION

In this paper, the principle and some practical aspects of proton-induced X-ray emission is presented. The applications of the method is reviewed with respect to quantitative analysis of trace elements of high or intermediate molecular weight in the biological material.

Introduction

Trace elements, that is elements which occur in a sample at concentrations of parts/million, play an important role in biological systems. In a living organism they are classified either as essential or non-essential even if this distinction is not always evident since it is bound to the sensitivity of the essay method. If more sensitive analytical methods were available many non-essential elements would probably be reclassified as essential. This would provide information of value in diagnosis and preventive medicine, since trace elements play an important role in many diseases [1, 2, 3].

It is known that the concentration of a single element is not particularly useful since this varies not only from person to person but from organ to organ and even within a single organ and it depends greatly on the homeostasis of the subject in examination. Knowledge of simultaneous concentrations of several elements is on the contrary very helpful since it has been observed experimentally that many correlations exist between es-

sential trace elements concentrations and the abnormal correlation values associated with pathological conditions (although the cause of that correlation is usually unknown) [4, 5, 6].

Any progress in this field of research is therefore conditioned by the development of highly sensitive analytical methods which permit the simultaneous determination of many trace elements.

At the National Laboratories of Legnaro we have studied the optimal conditions of some atomic and nuclear physics techniques which satisfy these requisites. The techniques studied were: proton-induced X-ray emission, elastic diffusion of α-particles and photon-induced X-ray fluorescence. The first two methods employ 7 MV and 2 MV Van de Graaff accelerators as sources of charged particles. The third method employs γ-emitter radioisotope sources to induce X-ray fluorescence in the samples.

The α-particles diffusion method needs thin targets of 10-20 $\mu g/cm^2$ of thickness. The possibility to detect several elements simultaneously depends on the mass resolution which can be optimized by an appropriate choice of the α-particle energy and detection angle. We observed that the method can be refined for the detection of light elements [7]; in this case the optimal working conditions involve the use of 5-10 MeV α-particles and 40-70° detection angles. Under these conditions the background contribution to the energy spectrum is usually negligible with biological matrices and it allows to reach detection limits of few hundred of ppm in 1 hour of measurement [7, 8].

The photon-induced X-ray fluorescence is optimized as the photon energy of the exiting source is lightly more than the binding energies of the K or L electron shells of the irradiated atom. Three sources as ^{55}Fe, ^{109}Cd and ^{241}Am, used alternatively, optimize the detection sensitivity for a large enough range of elements. The source activities are few millicurie. The source annular shaping allows to assemble a simple automatic facilitiy to perform several continuous measurements whose turns are controlled by a multichannel analyser [9]. This technique is particularly convenient in those experiments where a large quantity of samples has to be analysed and the required sensitivity is not high.

Eventually the proton-induced X-ray emission is a tool which couples the multielemental analysis for medium-heavy elements with a high sensitivity often superior to one reached by the neutron activation technique [10].

Pixe-experimental method

When a beam of charged particles penetrates a medium (the sample) electrons are ejected from the atomic orbits K, L, M, etc. with consequent emission of characteristic X-rays which are classified according to the orbit involved K_α, K_β, L_α, L_β, L_γ, etc. (Fig. 1). If the energy is measured with a suitable detector the elements in the sample may be deduced.

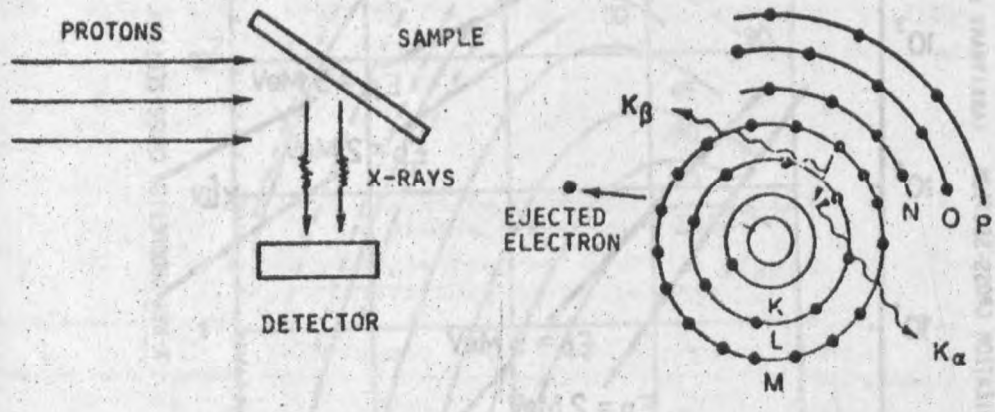

Fig. 1. Diagram showing the PIXE method and the characteristic X-ray production

Diagram przedstawiający metodę PIXE i wytwarzanie charakterystycznego promieniowania X

Slowing down in the sample the charged particles produce Bremsstrahlung and nuclear-γ radiation which originate the background. We shall see in the following that the background is competitive with respect to the characteristic X-rays in order to determine the sensitivity of the method.

Characteristic X-rays

The probability of X-ray emission for the i^{th} line σ_{Ei} is:

$$\sigma_{Ei} = \sigma_i \cdot \omega_i$$

where σ_i is the ionization probability of the i^{th} orbit (i = K, L, M, ...) and ω_i is the relative photon emission yield that is the ratio between the number of X-rays emitted and the number of ionizations occurred in the i^{th} orbit; ω_i is usually less than 1 because of the Auger effect.

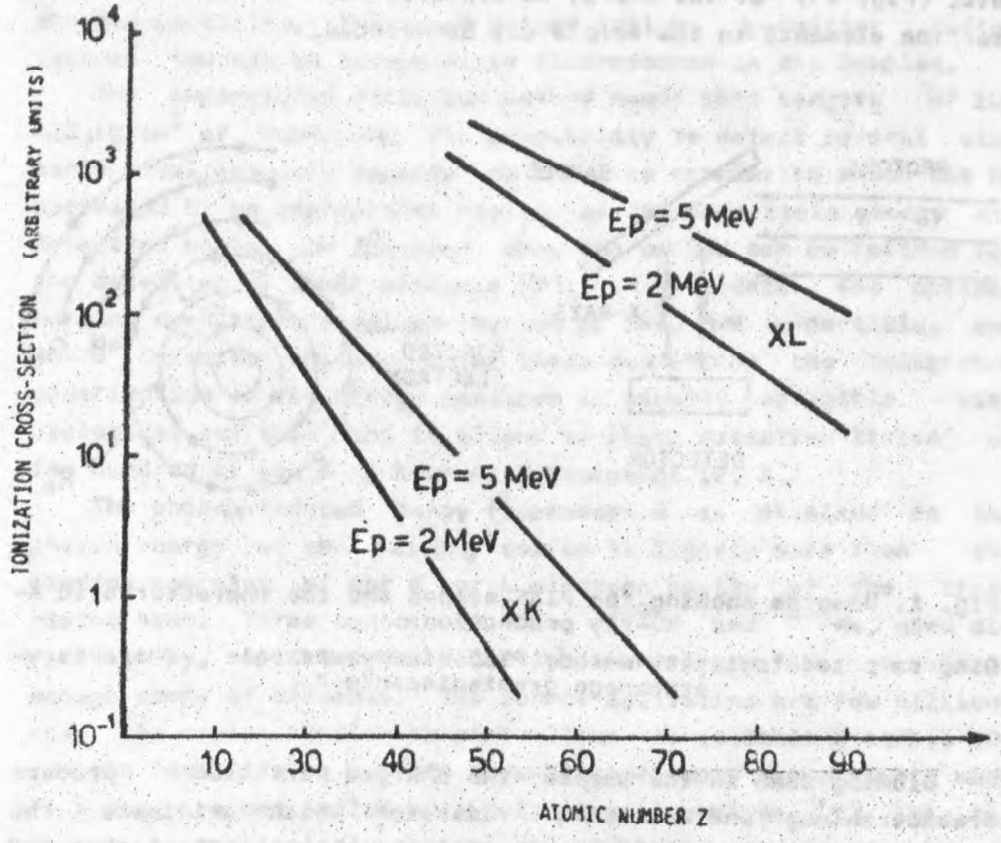

Fig. 2. Emission probability of XK- and XL-rays against the atomic number of target atom for two proton energies

Prawdopodobieństwo emisji promieniowania XK i XL jako funkcja liczby atomowej atomu - tarczy dla dwu wartości energii protonów

The X-ray yield depends on the atomic number of the target, the kind of particle used and on the particle energy. Taking into account protons as reference particles we can observe that the X-ray yield diminishes with the Z of the target and it is higher when more external orbits are involved (Fig. 2). The X-ray yield increases with the energy of the protons up to a maximum whose position depends on the target atomic number (Fig. 3).

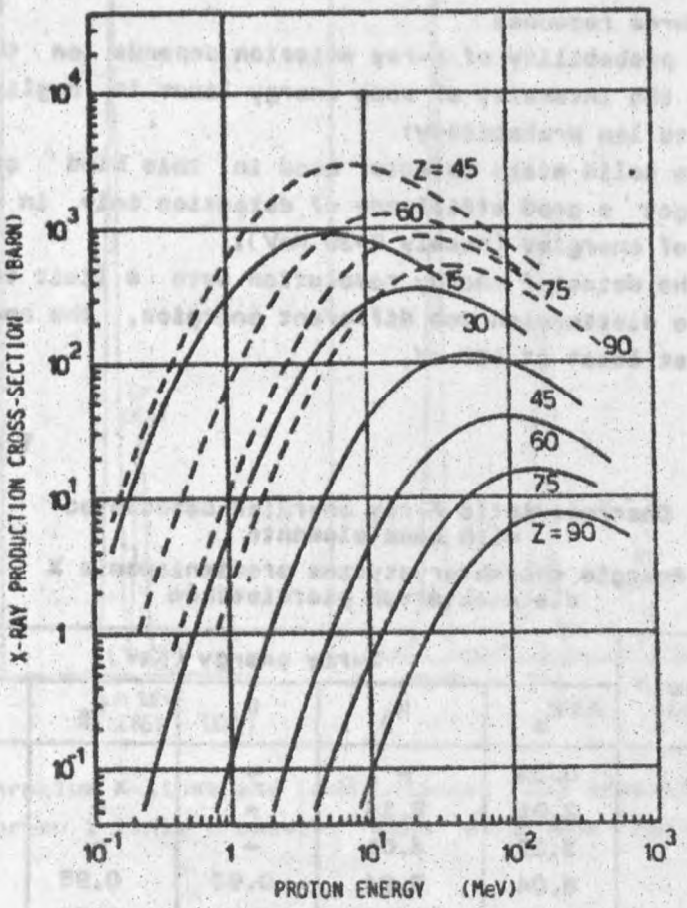

Fig. 3. XK and XL production cross-section against proton energy for atoms with different atomic number: (——) XK-rays, (---) XL-rays

Przekrój poprzeczny dla wytwarzanie promieniowania XK i XL jako funkcja energii protonu dla atomów o różnych liczbach atomowych: (——) promieniowanie XK, (---) promieniowanie XL

For heavier ions of atomic number z the X-ray production cross-section is proportional to z^2 multiplied by the cross-section of protons of the same velocity. This relationship is really valid only for ions lightly heavier than protons; for still heavier ions the characteristic X-ray yield shows resonances which do not exist in the proton cross-section.

The original X-ray spectrum may be very complicated specially for heavy elements, but the detected spectrum is simplified because of three reasons:

i) the probability of X-ray emission depends on the orbits involved, the intensity of some energy lines is negligible because of its low probability;

ii) the solid state detector used in this kind of experiments has got a good efficiency of detection only in a restricted range of energies (namely 2-30 KeV);

iii) the detector energy resolution sets a limit to the possibility to distinguish two different energies, the energy gap has to be at least of 150 eV.

T a b l e 1

Characteristic X-ray energies associated with some elements

Energie charakterystyczne promieniowania X dla niektórych pierwiastków

Elements	X-ray energy (KeV)				
	K_α	K_β	L_α	L_β	L_γ
N	0.39	-	-	-	-
P	2.01	2.14	-	-	-
Ca	3.69	4.01	-	-	-
Cu	8.04	8.94	0.93	0.95	-
As	10.52	11.79	1.28	1.32	-
Se	11.20	12.57	1.38	1.42	-
Cd	23.08	26.37	3.13	3.42	3.72
Hg	69.85	81.39	9.94	11.87	13.83
Pb	73.87	86.13	10.50	12.60	14.76
U	96.54	112.90	13.52	16.82	20.16

Consequently medium elements (15 < Z < 40) may be detected by the K-lines and heavy elements (Z > 40) by the L-lines. Table 1 gives the characteristic X-ray energies associated with some elements. Figure 4 shows Chromium K-lines and Lead L-lines as they are detected.

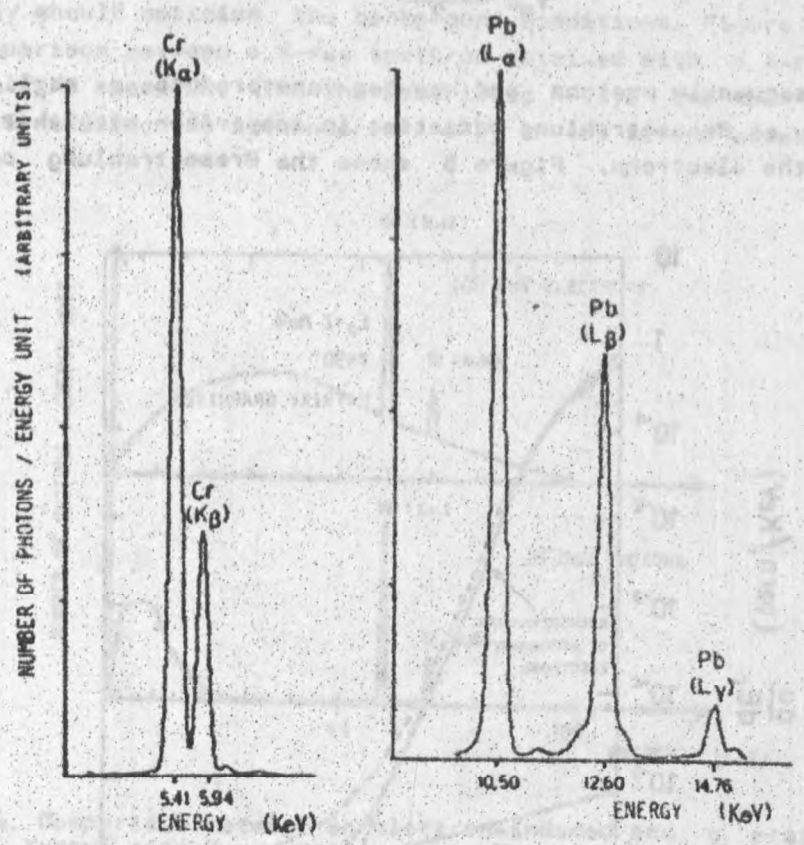

Fig. 4. Chromium K-lines and Lead L-lines. PIXE experimental data
Linie K chromu i linie L ołowiu. Dane otrzymane metodą PIXE

The background radiation

The background production is partly due to the γ-rays produced in the nuclear reactions which scatter in the target itself and dirty the X-ray spectrum, nevertheless it is mainly due to Bremsstrahlung radiation.

Whenever a charged particle slows down in the medium a continuous in energy electromagnetic radiation, called Bremsstrahlung, is emitted. The Bremsstrahlung yield depends both on the atomic number of the target (Z) and on the atomic number (z) and mass (m) of the projectile:

$$Y_B \propto \frac{Z^2 \cdot z^2}{m^2}$$

Consequently protons and heavier ions produce a negligible quantity of Bremsstrahlung radiation in comparison with that one due to the electrons. Figure 5 shows the Bremsstrahlung cross-

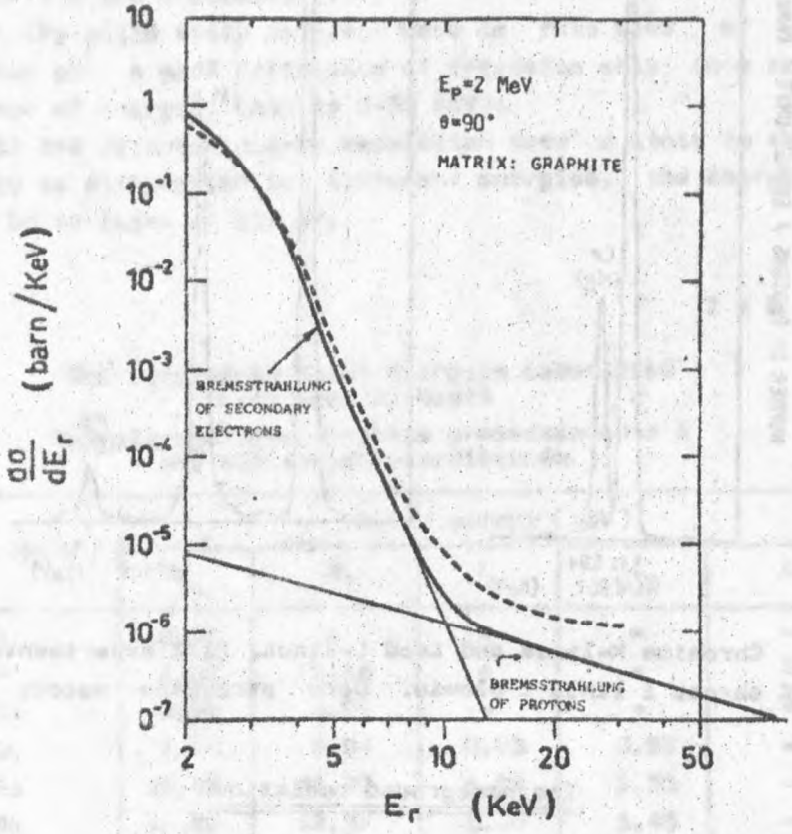

5. Bremsstrahlung cross-section for 2 MeV protons on graphite: (——) theoretical data, (---) experimental data

Przekrój poprzeczny dla wytwarzenia promieniowania hamowania na graficie dla protonów o energii 2 MeV: (——) dane teoretyczne, (---) dane doświadczalne

-section for a proton beam of 2 MeV of energy. The background is evidently due to the secondary electrons and it is negligible at energies bigger than 4 KeV.

In order to minimize the background radiation electron beams and sample matrices of high atomic number are not favoured. On the contrary biological samples and proton beams of few MeV of energy should optimize the background conditions. Figure 6 shows a comparison between a X-ray spectrum obtained with a X-ray tube and a PIXE spectrum. The characteristic X-rays and the background radiation do not interfere only in the second case.

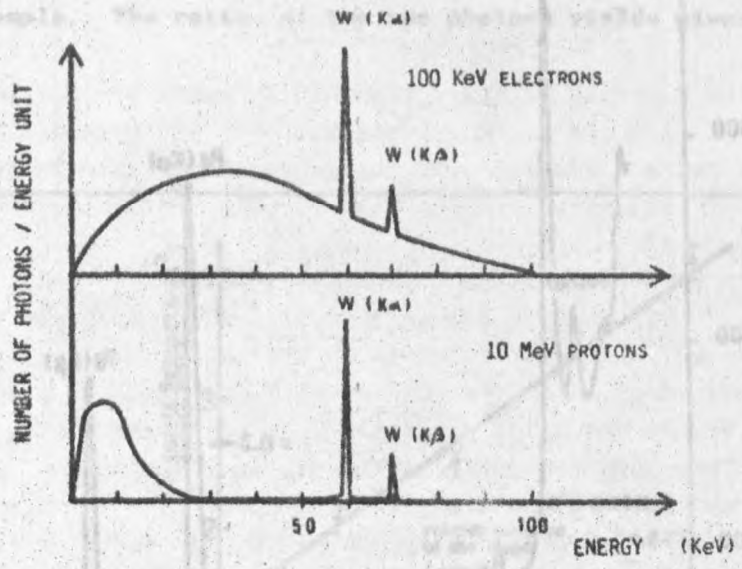

Fig. 6. Comparison between an electron-induced and a proton-induced X-ray spectrum of tungsten. The ordinate units are arbitrary

Porównanie widm promieniowania X wolframu indukowanego przez elektrony i indukowanego przez protony. Na osi rzędnych arbitralne jednostki

Quantitative analysis

In order to carry on a quantitative analysis of the trace element present in the sample the number of the emitted photons as well as several other parameters have to be known. If

one of the two following conditions is satisfied indeed:

i) uniformity of the beam:

ii) uniformity of the trace element distribution in the sample: then the number of X-ray emitted from the T element is:

$$(Nx)_T = N_{IN} \cdot \sigma_T \cdot C_T \cdot \xi_T$$

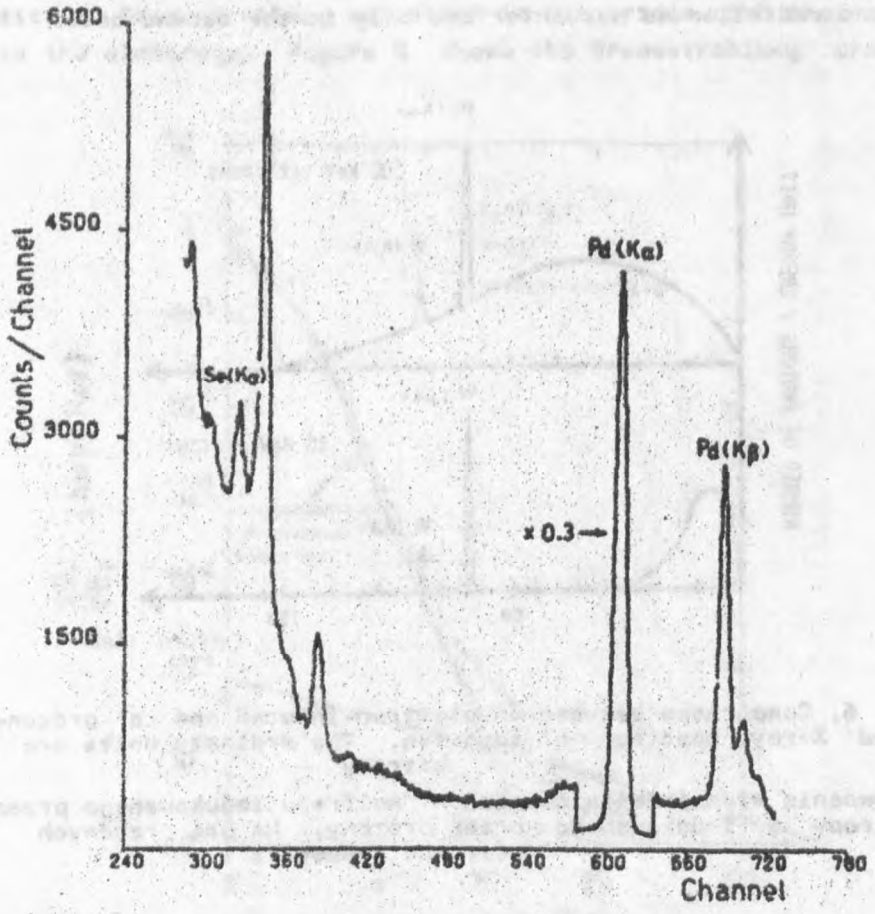

Fig. 7. Portion of a PIXE spectrum obtained at 1.8 MeV, with 250 nA proton beam in 100 min., on a self-supporting target of human blood serum. Pd is the internal standard (100 ppm as $PdCl_2$)

Część widma PIXE otrzymana dla 250 nA strumienia protonów o energii 1,8 MeV w ciągu 100 min., dla surowicy krwi ludzkiej jako samopodtrzymującej się tarczy. Jako standard wewnętrzny zastosowano Pd (100 ppm jako $PdCl_2$)

where: N_{IN} - is the number of incoming particles;
σ_T - is the probability of the X-ray emission;
C_T - is the concentration of the trace element in the sample;
ξ_T - is a coefficient which depends on the irradiation geometry, detection efficiency, X-ray absorption in the sample itself as well as along the path between the sample and the detector.

It is very difficult to have a good evaluation of ξ_T and also σ_T is poorly known, so the best method to determine C_T is to add a known quantity of an element S (the internal standard) in the sample. The ratio of the two photons yields gives:

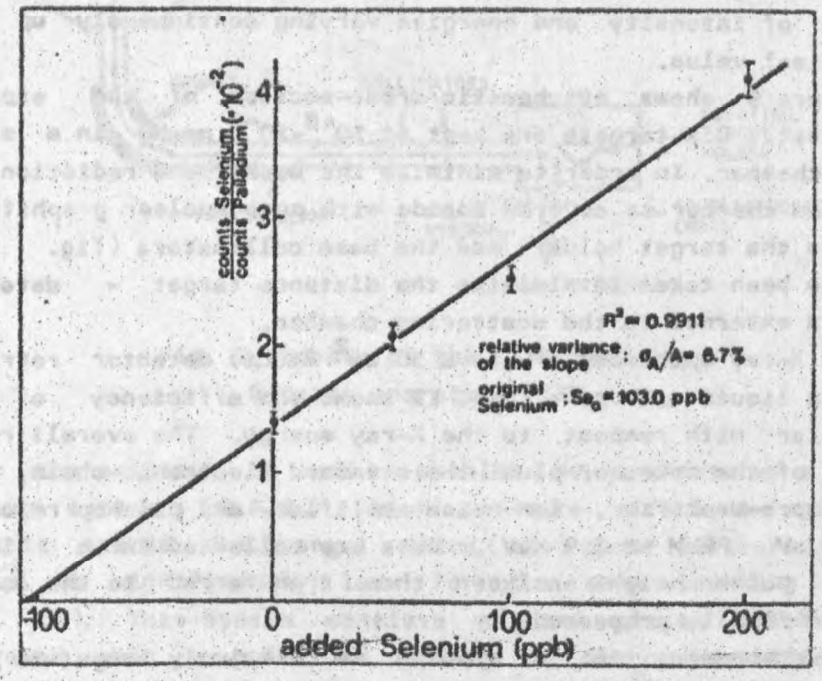

Fig. 8. Pellet calibration curve for Selenium. Proton beam energy: 1.8 MeV; sample: human blood serum. Pd is the internal standard

Krzywa kalibracyjna dla selenu. Energia strumienia protonów: 1 MeV; próbka: surowica krwi ludzkiej. Standard wewnętrzny: Pd

The quantity $K = \frac{\sigma_S \xi_S}{\sigma_T \xi_T}$ depends on the experimental set-up and on beam conditions, so it can be determined in a sample where C_T and C_S are known and then it becomes a constant of the experiment.

Figure 7 shows a piece of X-ray emission spectrum of a sample of human blood serum in which Selenium had to be measured, Palladium is the internal standard. By determining Se and Pd peak areas in different samples in which known quantities of Se are added the constant K is deduced from a calibration curve as in Fig. 8.

Experimental set-up

For the analysis of trace elements by means of PIXE the AN-2000 (2 MV) and CN (7 MV) accelerators of the National Laboratories of Legnaro are employed which provide proton beams up to few μA of intensity and energies varying continuously up to the maximal value.

Figure 9 shows a schematic cross-section of the experimental set. Six targets are kept at 10^{-5}-10^{-6} mm Hg in a scattering chamber. In order to minimize the background radiation the aluminium chamber is covered inside with pure nuclear graphite as well as the target holder and the beam collimators (fig. 10). Care has been taken to minimize the distance target - detector which is external to the scattering chamber.

The X-ray spectrometer is a 30 mm^2 Si(Li) detector refrigerated in liquid nitrogen: Fig. 11 shows the efficiency of such a detector with respect to the X-ray energy. The overall resolution of the detector plus the standard electronic chain, including pre-amplifier, low-noise amplifier and pile-up rejector, is 170 eV (FWHM at 5.9 KeV). Data are collected in a 1024-channel pulse height analyser then transferred to the computer and finally processed.

The processing time of a pulse is relatively large (~60 μs), consequently the pulse superposition risk is high at high counting rate. The pile-up rejector system (P.U.R.) avoids pulse superpositions which spoil the X-ray spectrum. In order to im-

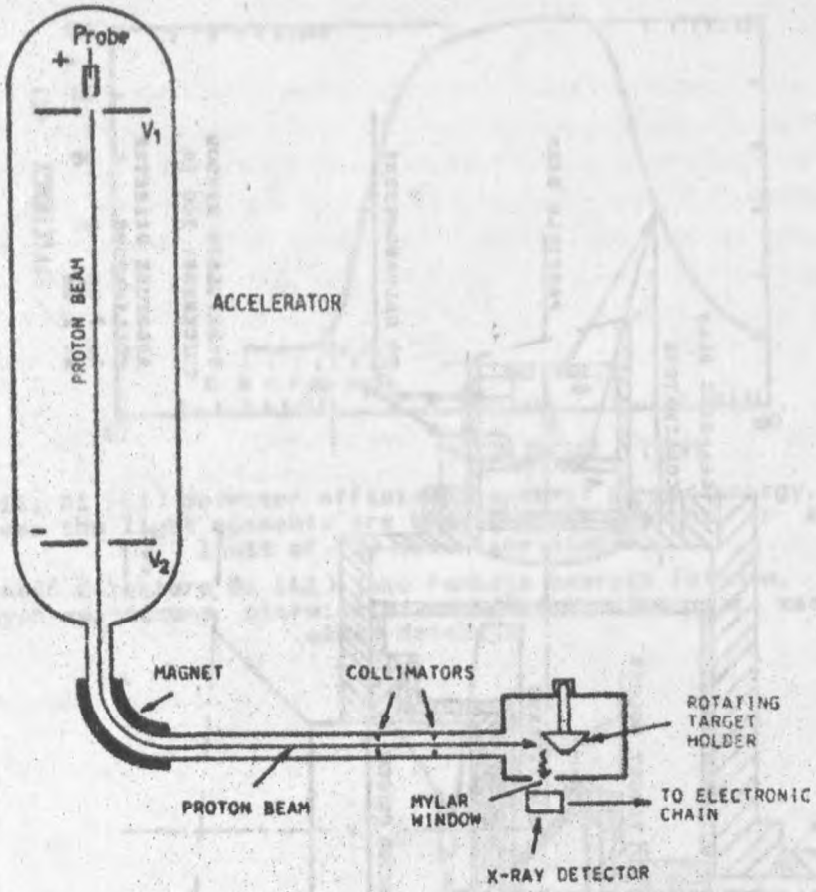

Fig. 9. Scheme of the PIXE facility
Schemat aparatury PIXE

prove the solution of such a problem we manufactured a beam pulsing system (B.P.S.) which is more efficient and moreover it spares the target since the power delivered in the sample is significantly less for the same counting rate (Fig. 12). This system consists of two plates which are polarized when a pulse is rising at the pre-amplifier output, in such a manner the incoming beam is bent out the scattering chamber.

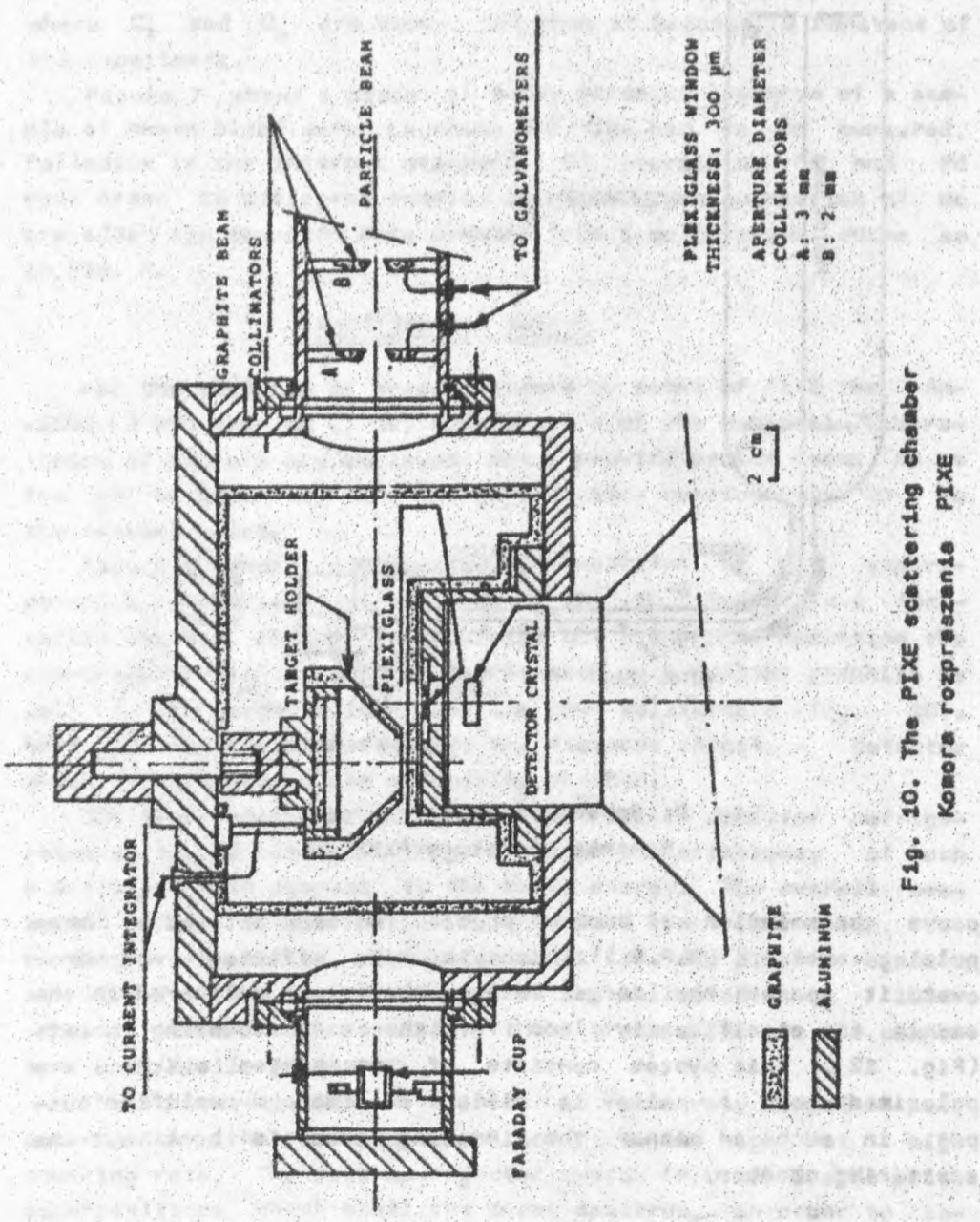

Fig. 10. The PIXE scattering chamber
Komora rozpraszania PIXE

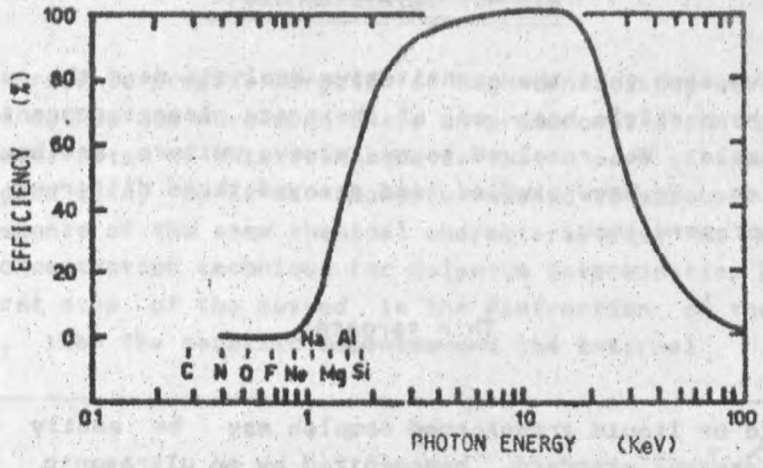

Fig. 11. Si (Li) detector efficiency against photon energy. In abeciesa the light elements are signed which are out or at the limit of the detection window

Wydajność detektora Si (Li) jako funkcja energii fotonów. Na osi rzędnych zaznaczono pierwiastki na granicy lub poza zasięgiem okna detekcji

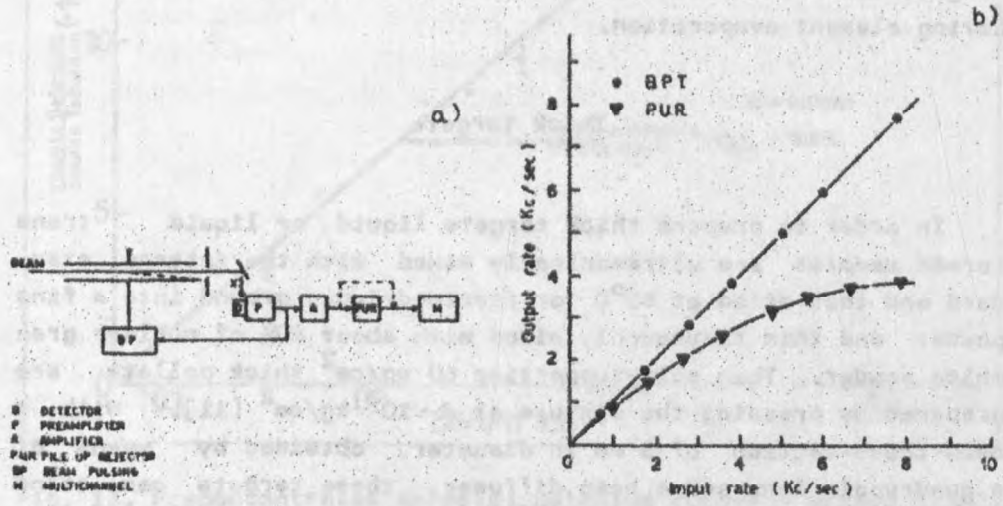

Fig. 12. Schematic drawing of the beam pulsing technique a) comparison between the beam pulsing and the pile-up rejector method, b) B.P.T. allows higher counting rates

Schemat techniki strumienia pulsacyjnego a) porównanie metody strumienia pulsacyjnego (B.P.T.) i metody "pile-up rejector"; b) metoda B.P.T. pozwala na wyższą szybkość liczenia

Sample preparation

We have seen that the quantitative analysis need the uniformity of the particle beam or of the trace element concentration in the sample. We resolved to use always uniform and homogeneous samples. We have studied and essayed three different methods to prepare them.

Thin targets

Liquid or liquid transformed samples may be easily dopped with an internal standard, homogenized by an ultrasonic probe and then sprayed with a nebulizer onto a formvar rotating backing which is in the meanwhile warmed up at about 40°C. In such a manner thin targets are prepared 20 $\mu g/cm^2$ thick. The homogeneity is assured when the droplets are so tiny to produce a less than 10 μm particulate on the formvar backing [7]. These targets can stand about 100 nA of proton beam without breaking or having element evaporation.

Thick targets

In order to prepare thick targets liquid or liquid transformed samples are ultrasonically mixed with the internal standard and then dried at 60°C or freeze-dried, ground into a fine powder and then thouroughly mixed with about 20% of nuclear graphite powder. Then self-supporting 60 mg/cm^2 thick pellets are prepared by pressing the mixture at $4 \cdot 10^3$ kg/cm^2 [11]. With a beam cross-section of 5 mm in diameter, obtained by means of a quadrupole lens and a beam diffuser, these targets can stand 500-600 nA of proton beam without element evaporation.

Preconcentrated targets

In order to prepare targets for high sensitivity measurements a third method was developed based on preconcentration techniques. A characteristic of this technique is that a part of trace elements gets lost, so it is a powerful method to measure one or few elements of the same chemical characteristics. We developed a preconcentration technique for Selenium determination [12, 13]. The first step of the method is the destruction of the organic matrix, then the metallic Selenium and the internal standard

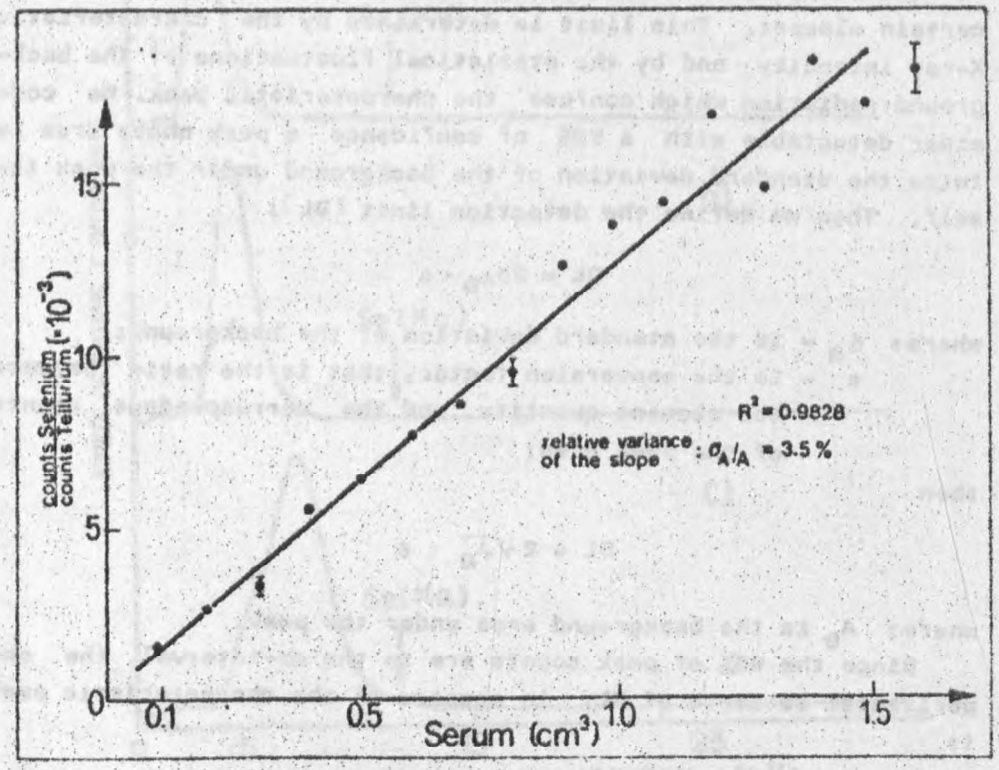

Fig. 13. Preconcentrated targets: Selenium recovery versus sample quantity (human blood serum). 1.8 MeV proton beam with 200 nA of current on a 5 mm in diameter spot

Tarcze wstępnie zagęszczone: odzysk selenu jako funkcja wielkości próbki (surowica krwi ludzkiej). Strumień protonów o energii 1,8 MeV, prąd 200 nA, średnica strumienia 5 mm

(Tellurium) are precipitated on a millipore filter which is then pressed on a Whatman filter. This technique has been applied to human blood serum and it has given a linear response between 0.1 and 2.0 cm^3 of serum (Fig. 13). These kinds of targets can stand 200-400 nA of proton beam without severe damage of the target itself or element evaporation.

Sensitivity

The detection limit is the minimum detectable quantity of a certain element. This limit is determined by the characteristic X-ray intensity and by the statistical fluctuations of the background radiation which confuse the characteristic peak. We consider detectable with a 95% of confidence a peak whose area is twice the standard deviation of the background under the peak itself. Then we define the detection limit (DL):

$$DL = 2\sigma_B \cdot \varepsilon$$

where: σ_B - is the standard deviation of the background;
ε - is the conversion factor, that is the ratio between the element quantity and the correspondent counts of the peak area;

then

$$DL = 2\sqrt{A_B} \cdot \varepsilon$$

where: A_B is the background area under the peak.

Since the 95% of peak counts are in the 4σ-interval, the experimental estimate of DL, in absence of the characteristic peak, is

$$DL = 2\sqrt{\int_{-2\sigma}^{+2\sigma} B} \cdot \varepsilon$$

or, with reference to the detection resolution and the relationship $FWHM = 2.354 \cdot \sigma$.

$$DL = 2\sqrt{\int_{-0.85\ FWHM}^{+0.85\ FWHM} B} \cdot \varepsilon \qquad (1)$$

Note that the background increases with the time t. If the beam current is constant, ε decreases as 1/t, so DL decreases with the inverse root of the time of measurement:

$$DL \equiv DL\left(\frac{1}{\sqrt{t}}\right)$$

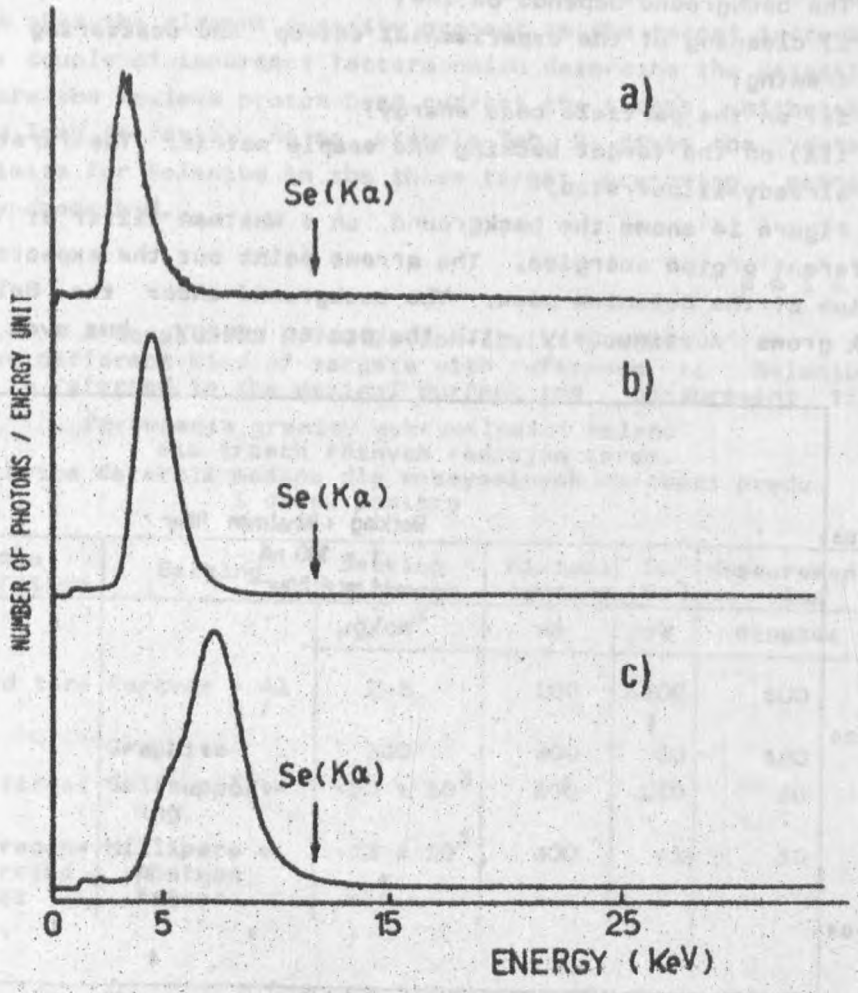

Fig. 14. Bremsstrahlung backgrounds of Whatman blank targets at different proton energies: a) 1.8 MeV; b) 3.0 MeV; c) 4.0 MeV. At 11.2 KeV there is the expected Selenium peak. Ordinate units are arbitrary

Tło promieniowania hamowania na wzorcowych tarczach Whatman'a dla wyższych energii protonów
a) 1,8 MeV; b) 3,0 MeV; c) 4,0 MeV. Oczekiwany szczyt selenu przy 11,2 KeV. Na osi rzędnych arbitralne jednostki

Considered the conversion factor a constant of the experiment, the relationship 1 shows that the detection limit depends on the background B and on the detector-electronic chain resolution FWHM. A good detector and a good electronic chain optimize quite easily the FWHM, then the background minimizing remains the unique task in order to have the best sensitivity.

The background depends on the:

i) cleaning of the experimental set-up and scattering chamber drawing;

ii) on the particle beam energy;

iii) on the target backing and sample matrix. The first item was already illustrated.

Figure 14 shows the background on a Whatman filter at three different proton energies. The arrows point out the expected position of the Selenium peak. The background under the Selenium peak grows continuously with the proton energy, but even the

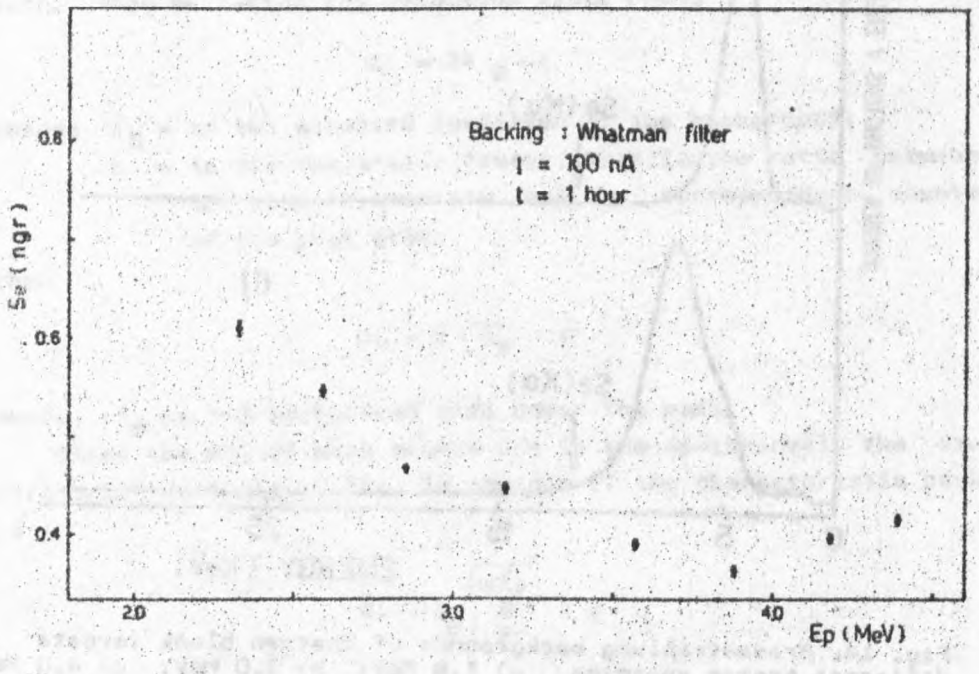

Fig. 15. Detection limit of Selenium as a function of proton energy (confidence level: 95%)

Granica wykrywalności selenu jako funkcja energii protonu (poziom ufności 95%)

characteristic X-ray yield increases up to a maximum (Fig. 3). So the detection limit is expected to have a minimum with respect to the proton energy. Figure 15 shows this minimum for Selenium.

Biological matrices and graphite backing minimize the background because of their low atomic number. Thin targets are better than thick targets from this point of view, but the detection limit depends even on the conversion factor ε, which decreases when the element quantity present in the target increases. Another couple of important factors which determine the detection limit are the maximum proton beam current the target withstands and how long it lasts. As an example Tab. 2 gives the detection limits for Selenium in the three target preparing methods already described.

T a b l e 2

A comparison of detection limits reached by three different kind of targets with reference to Selenium. The DL is referred to the maximal current and measurement time

Porównanie granicy wykrywalności selenu dla trzech różnych rodzajów tarcz. Granica detekcji podana dla maksymalnych wartości prądu i czasu pomiaru

Sample preparation	Backing	Backing thickness	Maximal current	DL (Se)	Measurement time
		$\mu g/cm^2$	nA	ppb	minutes
Sprayed target	Formvar + Al	2-5	100	≥100	600
	Graphite	300	400	80	180
Thick target	Selfsupporting	$\sim 60 \times 10^3$	600	≤10	60
Thin preconcentrated target	Millipore + Whatman filter	$\sim 13 \times 10^3$	300	<1	10

Conclusions

The Proton-Induced X-ray Emission is a powerful method to detect quantitatively trace elements of medium-high atomic number; however it needs care both for the experimental set-up and the target preparation in order to exploit all the possibilities of the method.

REFERENCES

[1] Bowen H. J. M., Trace Elements in Biochemistry, London-New York (1967).

[2] Hueper W. C., Conway W. D., Chemical Carcinogenesis and Cancers, Springfield, Illinois (1964).

[3] Schwarz K., The Role of Trace Elements in Health and Disease Process in Man and Animals, with Special Reference to Elements Newly Identified as Essential, IAEA/SM-157/80.

[4] Schicha H., Kasperek K., Riedel V., Feinendegen L. E., Vyska K., Müller W., Trace Elements in Normal Mammalian Tissue and Corresponding Malignant Tumours, IAEA/SM-157/37.

[5] Underwood E. J., Trace Elements in Human and Animal Nutrition, New York-London (1971).

[6] Wills C. F., [in:] Proceedings of WAAP/IBP, Internat. Symp. Livingstone, Edinburgh-London (1970).

[7] Colautti P., Moschini G., Stievano B. M., J. Radioanal. Chem. 34, 171 (1976).

[8] Colautti P., Enzi G., Moschini G., Muzzio P. C., Stievano B. M., La Ricerca Clin. Lab. 6, 170 (1976).

[9] Lazzarini L., Moschini G., Stievano B. M., [in:] Quaderno della Soprintendenza ai Beni Artistici e Storici di Venezia, Nuova Serie, n. 9, giugno (1980).

[10] Falkman F., Gaarde C., Huus T., Kemp K., Nucl. Instr. and Meth. 116, 487 (1974).

[11] Berti M., Buso G., Colautti P., Moschini G., Stievano B. M., Tregnaghi C., Anal. Chem. 49, 1313 (1977).

[12] Buso G. P., Colautti P., Moschini G., Stievano B. M., Acta Medica (1982).

[13] Buso G. P., Colautti P., Moschini G., Stievano B. M., High Sensitivity PIXE Determination of Selenium in Biological Sample Using a Pre-

concentration Technique; 3rd Intern. Conf. on PIXE, Heidelberg 18-22 July 1983.

Laboratori Nazionali
dell'Instituto Nazionale
di Fisica Nucleare, Legnaro, Italia
Instituto di Fisica
G. Galilei dell'Università di Padova

G. Bueo, P. Colautti, G. Moschini, B. M. Stievano

JĄDROWA TECHNIKA ILOŚCIOWEJ ANALIZY ELEMENTARNEJ: EMISJA PROMIENI X INDUKOWANA PRZEZ PROTONY

W artykule przedstawiono zasadę oraz omówiono niektóre aspekty praktyczne zjawiska emisji promieni X, indukowanej przez protony w zastosowaniu do ilościowej analizy pierwiastków śladowych o wysokich lub średnich masach cząsteczkowych w materiale biologicznym.